IAC–16–C1.9.1

PERIODIC ORBIT-ATTITUDE SOLUTIONS ALONG PLANAR ORBITS IN A PERTURBED CIRCULAR RESTRICTED THREE-BODY PROBLEM FOR THE EARTH-MOON SYSTEM

Lorenzo Bucci and Michèle Lavagna
Politecnico di Milano, Italy
lorenzo.bucci@mail.polimi.it, michelle.lavagna@polimi.it

Davide Guzzetti and Kathleen C. Howell
Purdue University, United States
dguzzett@purdue.edu, howell@purdue.edu

Interest on Large Space Structures (LSS), orbiting in strategic and possibly long-term stable locations, is nowadays increasing in the space community. LSS can serve as strategic outpost to support a variety of manned and unmanned mission, or may carry scientific payloads to broaden the knowledge of our universe. The paper is devoted to the analysis of LSS in the Earth-Moon system, exploiting the dynamics offered a multi-body gravitational environment. The coupling between attitude and orbital dynamics is investigated, with particular interest on the gravity gradient torque exerted by the two massive attractors. First, natural periodic orbit-attitude solutions are obtained; a LSS that exploits such solutions would benefit of a naturally periodic body rotation synchronous with the orbital motion, easing the effort of the attitude control system to satisfy pointing requirements. Then, the solar radiation pressure is introduced into the fully coupled dynamical model and its effects investigated, discovering novel periodic attitude solutions. Benefits of periodic behaviors that incorporate solar radiation pressure are discussed, and analyzed via the variation of some parameters (e.g reflection/absorption coefficients, position of the center of pressure). As a final step to refine the current perturbed orbit-attitude model, a structure flexibility is also superimposed to a reference orbit-attitude rigid body motion via a simple, yet, effective model. The coupling of structural vibrations and attitude motion is preliminarily explored, drawing conclusions on possible challenges faced by LSS.

I. Introduction

Nowadays, the Earth-Moon system is attracting more and more interest as a well suited location for near, and far future, long term missions for Large Space Structures (LSS). The design process for LSS goes beyond the sole trajectory definition, and a deep understanding of the orbital and attitude coupled motions is warranted; interesting dynamical structures underlie the orbit-attitude coupled problem, and periodic orbit-attitude solutions may be found. A vehicle which exploits a natural periodic attitude behavior may allow to relieve some of the control effort from the Attitude Control System (ACS), for example, by satisfying coarse pointing requirements via passive stabilization.

Pioneering studies [1, 2] and more recent researches [3, 4] investigate the dynamics of a rigid body at a Lagrangian point; Wong et al. [5] also introduce the coupling between small, linearized orbital motion and attitude dynamics, presenting resonance conditions.

More recent investigations are devoted to the fully coupled orbital-attitude dynamics. Guzzetti and Howell [6, 7, 8] identify orbit-attitude periodic solutions for planar orbits, providing a distinction between elementary planar motions and three-dimensional solutions; Knutson et al. investigate the rigid body motion that is associate with planar [9] and three-dimensional [10, 11] orbits, identifying bounded and unbounded attitude responses. A wide range of techniques to search, identify and exploit coupled orbit-attitude behaviors for space mission design is provided by Guzzetti [12].

The scope of the present work is a deeper analysis of the coupled orbit-attitude motion in the Earth-Moon system, aiming to map the solution space and to define a framework for the operational exploitation of such solutions. A correct utilization of periodic behaviors may, in fact, be an aid to the ACS for a space vehicle that operates in a multi-attractor gravitational environment, and it may open new scenarios for mission design.

The paper is organized as follows: Section II provides the models and the nomenclature used for the analysis; Section III presents periodic orbit-attitude solutions and their classification into families, leveraging a graphical mapping of the solution space; Section IV further elaborates the dynamical model, introducing the effect of Solar Radiation Pressure (SRP) and demonstrating novel periodic solutions, ones that exploit the SRP torque; Section V investigates the effect of structural flexibility on attitude motions obtained under the rigid body approximation, fostering the application of periodic solutions to real space structures.

II. Model and assumptions

II.I Equations of motion

Let us consider a rigid spacecraft, with an attached principal inertia frame $\hat{x}_b\hat{y}_b\hat{z}_b$, moving under the gravitational pull of two massive attractors m_1 and m_2, called primaries. The translational dynamics is conveniently described in a rotating frame $\hat{X}_s\hat{Y}_s\hat{Z}_s$, whose angular velocity equals the relative mean motion of the two primaries, depicted in Figure 1; $\mathbf{r}_1$ and $\mathbf{r}_2$ represent the position of the spacecraft with respect to the primaries. This problem is known as the Circular Restricted Three-Body Problem (CR3BP).

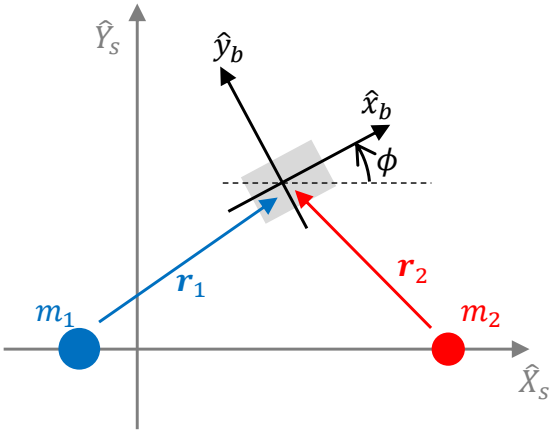

Figure 1: Reference frames

Equations of motion are conveniently normalized with respect to the time, length and mass units of the primary system [13];

$$\ddot{x} - 2\dot{y} - x = -\frac{1-\mu}{r_1^3}(x+\mu) - \frac{\mu}{r_2^3}(x-1+\mu) \quad (1)$$

$$\ddot{y} + 2\dot{x} - y = -\frac{1-\mu}{r_1^3}y - \frac{\mu}{r_2^3}y \quad (2)$$

r_1 and r_2 denote the norm of $\mathbf{r}_1$ and $\mathbf{r}_2$, respectively. The resulting set of equations (1),(2) is governed by a single parameter, called mass ratio, defined as

$$\mu = \frac{m_2}{m_1 + m_2} \quad (3)$$

Although the CR3BP does not possess a closed-form solution, five relative equilibrium points are known. Families of periodic trajectories (in the rotating frame) emanate from the proximity of the these equilibria, where the centrifugal and gravitational forces null each other. The equilibrium points, also called Lagrangian points, are depicted within the rotating frame in Figure 2, where d denotes the length unit of the system, i.e. the Earth-Moon distance. The three points lying on the X_s-axis of the rotating frame are usually called collinear Lagrangian points.

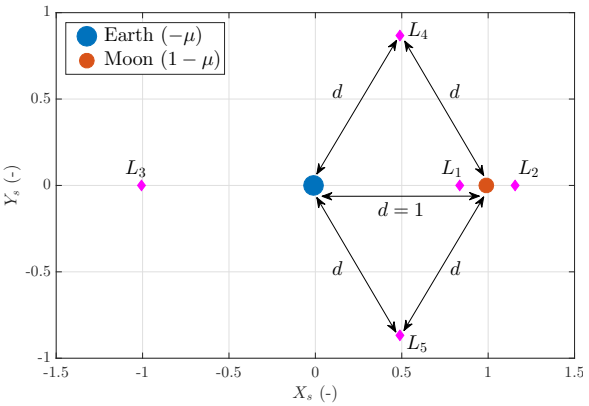

Figure 2: Equilibrium points in the Earth-Moon CR3BP

Planar rotational dynamics is described by Euler's equation about $\hat{z}_b$ direction, which coincides with the $\hat{Z}_s$ axis.

$$\dot{\omega}_z = 3\frac{I_y - I_x}{I_z}\left(\frac{1-\mu}{r_1^3}e_1e_2 + \frac{\mu}{r_2^3}l_1l_2\right) \quad (4)$$

I_x, I_y and I_z in equation (4) denote the principal inertia moments of the spacecraft, about the center of mass, in the principal inertia frame $\hat{x}_b\hat{y}_b\hat{z}_b$; e_1e_2 and l_1l_2 are the direction cosines of $\mathbf{r}_1$ and $\mathbf{r}_2$, respectively, in body axes; the right-hand term denotes the gravity gradient torque exerted by the two primaries [4].

Observing equation (4), the inertia topology for the spacecraft, in the planar dynamics, may be described through a coefficient K_z, which is called inertia ratio, defined as follows

$$K_z = \frac{I_y - I_x}{I_z} \quad , \quad (5)$$

Considering a planar case only, the rotation of the spacecraft may be represented by a single parameter; the angle between $\hat{x}_b$ and X_s axes, ϕ, is selected to represent the spacecraft orientation. Positive angles are measured in counterclockwise direction, as plotted in Figure 1.

II.II Families of orbit

Within the CR3BP, a large variety of planar periodic motions are accessible, along with a vast literature that discusses numerical techniques to produce those solutions [14]. Figure 3 portrays a sample of planar orbit families that are often proposed as a final destination for lunar exploration, or as a staging location for interplanetary missions. Accordingly, the present analysis focuses on this type of trajectories.

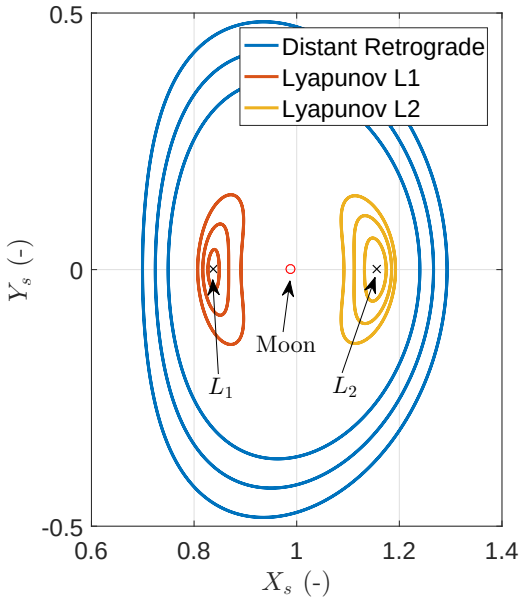

Figure 3: Planar CR3BP orbit families

Planar Lyapunov orbits branch out from the collinear Lagrangian points towards the primaries; a few Lyapunov orbits around L_1 and L_2 are depicted in Figure 3. The L_2 orbits might be suitable for translunar infrastructures to support interplanetary travels and lunar activities, while orbits around L_1 could be exploited to ease transfers from Earth to lunar orbits and back [15, 16]. Distant Retrograde Orbits (DRO) are particularly appealing for lunar missions design for their high degree of stability [17, 18]; in addition, these orbits encircle both Lagrangian points L_1 and L_2 and may exploit other orbits transfer manifolds to and from other orbit families [15]; DROs are also among the possible parking orbits considered for NASA's Asteroid Redirect Mission [19].

III. Periodic orbit-attitude solutions

The exploitation of the dynamical coupling between orbit and attitude motion may offer operational possibilities for space mission design. Before including additional external perturbations, the orbit-attitude coupled dynamics for a rigid body are explored with the extension of the gravity action to the attitude motion. Periodic orbit-attitude solutions exist in the planar CR3BP; such solutions are a peculiar combination of translational and angular motion, where the dynamical behavior repeats at regular intervals both in the trajectory and in the attitude response.

III.I Model and algorithm

To identify periodic orbit-attitude solutions a search method needs to be defined. The search method is developed on the assumption of a rigid spacecraft traveling within an unperturbed CR3BP, where forces and torques are only induced by the gravitation pull exerted by the two primaries. Kane [20] provides an expression to compute the acceleration induced by a massive attractor on the center of mass of an extended rigid body; the extended rigid body acceleration may be negligible with respect to other significant perturbations [18], and, accordingly, it is excluded from the present dynamical model. No modifications are then applied to equations (1) and (2).

An algorithm to search for a periodic orbit-attitude solution may be summarized in the following steps:

1. A periodic orbit is obtained, using standard differential correction techniques and well-known initial conditions;

2. The spacecraft topology is defined through the parameter K_z;

3. The attitude motion is propagated along one orbital period T, for a given span of initial body angular velocities $\omega_z(0)$, starting with body axes aligned with the rotating frame;

4. For each value of $\omega_z(0)$, the angular velocity $\omega_z(T)$ and rotation angle $\phi(T)$ after one orbit period are collected, and the variations with

respect to initial conditions $\Delta\omega_z, \Delta\phi$ are computed*

$$\Delta\omega_z = \omega_z(T) - \omega_z(0) \qquad \Delta\phi = \phi(T) \qquad (6)$$

5. A periodic solution is identified when both $\Delta\omega_z$ and $\Delta\phi$ are simultaneously null (within a tolerance of 10^{-9} non-dimensional units).

A graphical example of the algorithm rationale is depicted in Figure 4 (the term "periodic solution" refers to the value of $\omega_z(0)$ which is necessary, for a given orbit, to establish a periodic planar attitude motion).

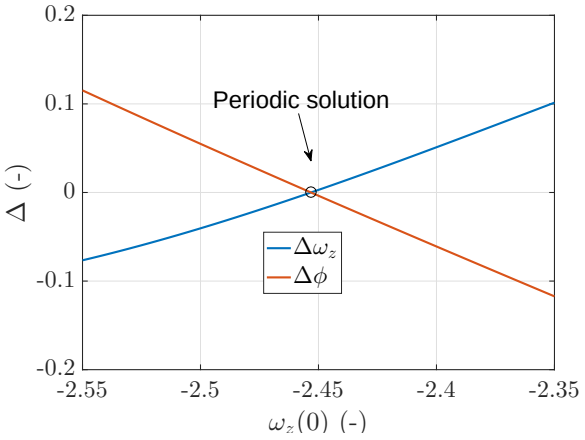

Figure 4: Periodic solution search algorithm

Guzzetti and Howell [7, 8] describe a different algorithm to obtain periodic orbit-attitude solutions, one that leverages a differential correction update for both the spatial orbit and attitude motions to achieve periodicity. The present algorithm fixes the operational orbit and specializes on periodic attitude behaviors strictly associated to a given trajectory.

III.II Families of solutions

Considering a planar periodic orbit, there exist multiple values of $\omega_z(0)$ that guarantee a periodic, planar rotational motion, as noted in [21] during the study of distant retrograde orbits. In general, for the type of solutions currently identified, an initial angular velocity corresponds to N spacecraft rotations, about its $\hat{z}_b$ axis, any one orbit revolution; this observation yields a classification of the solutions into families, each characterized by its own N.

Figure 5 portrays attitude periodic families for DROs, and considering a vehicle with $K_z = 0.8$. The reference periodic trajectory is represented along the

*Recall that $\phi(0) = 0$ since $\hat{x}_b$ coincides with $\hat{X}_s$.

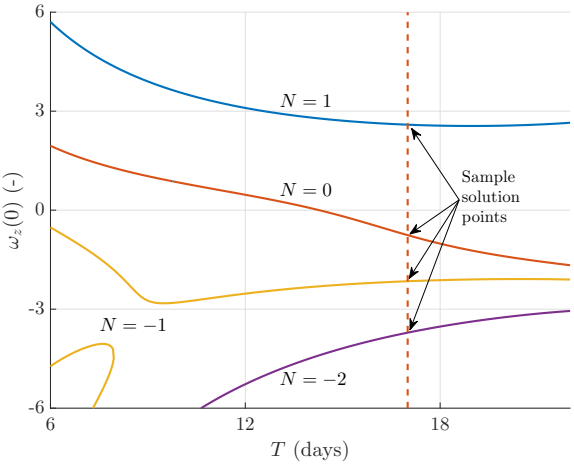

Figure 5: Solution families for DROs, $K_z = 0.8$

horizontal axis, identified by its period; the vertical axis corresponds to the initial angular velocity $\omega_z(0)$, that generates a periodic attitude behavior, superposed to the reference orbital motion. Different lines correspond to the different attitude families.

A set of sample solutions is depicted in Figure 6, including time histories for the rotation angle and the body angular velocity for a DRO with period of 17 days. In Figure 6, each line renders a different family of attitude periodic solution, as indicated my the number of rotations, N. This solution profile matches the results obtained by Guzzetti [12].

III.III Attitude periodicity maps

Once the attitude periodic solutions are identified and classified into families, it is possible to step forward in mapping the solution space. Families of solutions exist for different values of inertia ratio K_z, and may be, thus, plotted together to visualize a more informative picture of the solution set.

Recall that, an identification effort for periodic attitude solutions is necessarily tied to the model, and classification, employed. That is, for the current work, a planar attitude behavior where the body carries out an integer number, N, of rotations per orbit. Other orbit-attitude solutions exist, both in the planar and three-dimensional case [12], and might be further explored and classified.

Attitude periodicity maps represent an useful tool to graphically depict the orbit-attitude solution space. For example, Figure 7 portrays an attitude periodicity map for DROs, considering the whole span of K_z values.

Figures 8 and 9 depict, respectively, attitude peri-

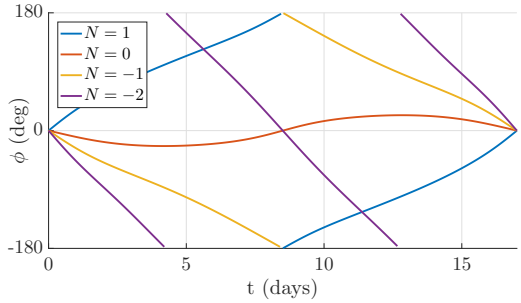

(a) Rotation angle

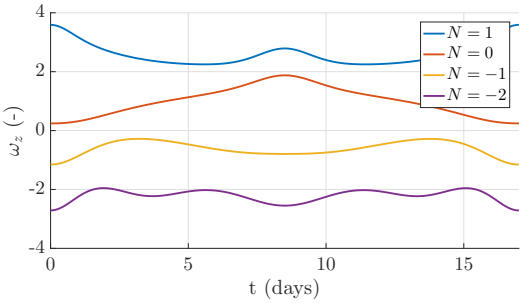

(b) Angular velocity

Figure 6: Sample periodic solution $K_z = 0.8$, DRO with $T = 17$ days

odicity maps for planar Lyapunov orbits around the Lagrangian points L_1 and L_2.

Note that, the $K_z = 0$ case is equivalent to a planar torque-free motion, since such mass distribution would not experience any attitude perturbation due to gravity gradient. Thus, the periodic solutions for $K_z = 0$ correspond to a trivially commensurate orbit-attitude motion, produced by an initial condition $\omega_z(0) = \frac{2\pi N}{T}$, where T is the orbital period.

IV. Effect of solar radiation pressure

The gravity gradient torque strongly affects the rotational motion of a rigid body, but in a CR3BP environment it may not be the largest in magnitude. In particular, large space structures with extended surfaces (e.g. solar arrays) are subjected to a large force generated by the Solar Radiation Pressure (SRP). The SRP force generally perturbs both the orbital path and the attitude motion; SRP produces, in fact, an acceleration on the vehicle center of mass, and, also, a torque, when there exists a lever between the solar radiation center of pressure and the spacecraft center of mass. Since an additional SRP moment may largely perturb a periodic attitude solution, that is available within a simplified gravitational model, the

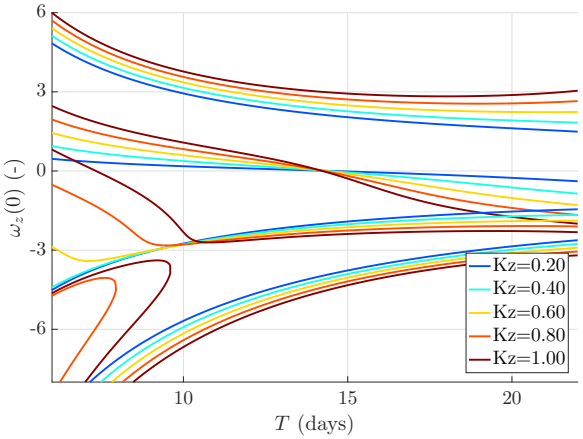

Figure 7: Periodicity maps for Distant Retrograde Orbits

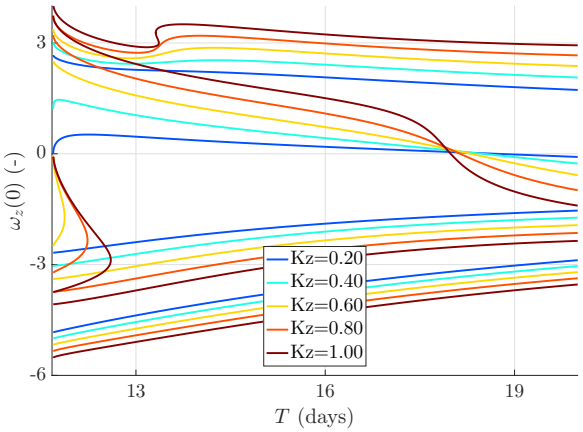

Figure 8: Periodicity maps for L_1 Lyapunov orbits

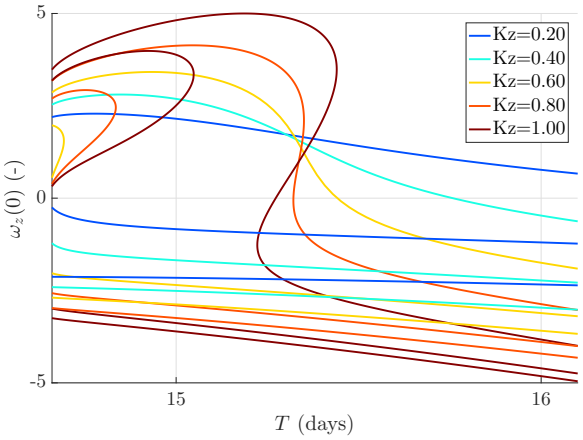

Figure 9: Periodicity maps for L_2 Lyapunov orbits

inclusion of SRP in the framework is warranted.

This investigation only includes the torque component of SRP, while the effects for the acceleration are neglected, assuming an unperturbed reference trajectory. This simplification, in general, is not a sufficiently accurate representation for the actual natural motion, however, a station-keeping system is typically employed to maintain the nominal path in real mission applications.

IV.I Model for solar radiation pressure

Consider an infinitesimal surface dA, subject to an incoming Sun radiation flux W_0 (e.g., $\simeq$1361 W/m^2 in the Earth-Moon system). The infinitesimal force generated by SRP [22] may be written as

$$d\mathbf{F}_{SRP} = -\frac{W_0}{c_0} dA(\hat{s}\cdot\hat{n})\Big[2C_s|\hat{s}\cdot\hat{n}|\hat{n} + C_d\left(\frac{2}{3}\hat{n}+\hat{s}\right) + C_a\hat{s}\Big] \quad (7)$$

depending on the fraction of radiation reflected specularly (C_s), diffusively (C_d) or absorbed (C_a). The symbol $\hat{s}$ denotes the Sun direction, $\hat{n}$ indicates the direction of the normal to the surface dA, whereas c_0 is the speed of light in vacuum; in the case of an opaque surface, note that the three coefficients C_s, C_a, C_d satisfy the following identity

$$C_s + C_a + C_d = 1 \quad (8)$$

so that only two coefficients are sufficient to fully describe an SRP interaction.

For a preliminary analysis including the SRP torque along orbit-attitude periodic solutions, it is convenient to lump all the external area of the spacecraft into a single flat surface A, whose normal $\hat{n}$ is known in the $\hat{x}_b\hat{y}_b\hat{z}_b$ frame [21]. Such surface is exposed to radiation on both sides, so that the total force acting on the spacecraft may be reduced to

$$\mathbf{F}_{SRP} = -\frac{W_0}{c_0} A(\hat{s}\cdot\hat{n})\Big[(1-C_s)\hat{s} + \left(2C_s|\hat{s}\cdot\hat{n}| + \frac{2}{3}(1-C_s-C_a)\right)\hat{n}\Big] \quad (9)$$

Within a lumped-area approach, the SRP torque may be modeled through the knowledge of the position $\mathbf{d}_c$ of the center of pressure with respect to the center of mass; by assumption, $\mathbf{d}_c$ is fixed in the principal inertia frame. The total torque due to SRP, thus, results in

$$\mathbf{T}_{SRP} = \mathbf{d}_c \times \mathbf{F}_{SRP} \quad (10)$$

In the present planar case, both $\mathbf{d}_c$ and $\mathbf{F}_{SRP}$ lie in the $\hat{X}_s\hat{Y}_s$ plane, so the resulting torque vector is directed as $\hat{Z}_s$.

IV.II Sun motion model

The relative direction of the Sun within the Earth-Moon system may be described, as a first approximation [23], assuming an apparent planar motion within the $\hat{X}_s\hat{Y}_s$ plane, and with constant angular velocity Ω_{sun}. The angle, θ_{sun}, between the Sun and the $\hat{X}_s$ axis is, then, a linear function of time. Figure 10 portrays the Sun position obtained within such a simplified model. Additionally, when the Sun radiation reaches the Earth-Moon system, it is approximated by a parallel beam ray.

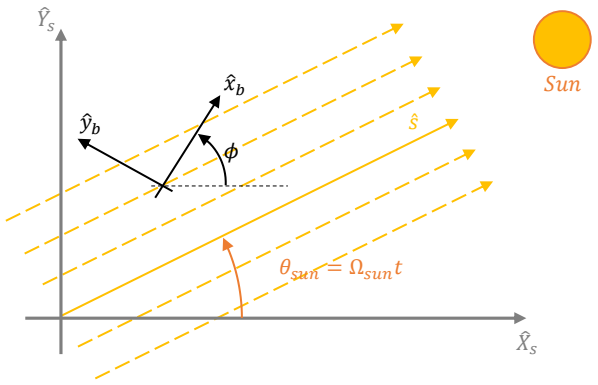

Figure 10: Apparent Sun motion in the CR3BP

Since the principal objective is to investigate periodic orbit-attitude solution, the inclusion of SRP generates a periodic excitation, whose period depends on the relationship between the orbital period and that of the apparent Sun motion. If an integer ratio exists between the reference trajectory period and the SRP action, a periodic solution may exist, one that is both commensurate (with different ratio) to the apparent motion of the Sun, and to the orbit period.

The study focuses then on planar orbits whose period is a submultiple of the apparent Sun period, called Sun-resonant orbits. Most of the attention will be devoted to the 1:2 resonance, i.e., the orbits where the spacecraft carries out two orbital revolutions, while the apparent Sun revolves once. Such resonance exists both for DROs and Lyapunov orbits.

IV.III Modified periodic solutions

The search for a periodic attitude solution is extended to an SRP-perturbed environment. If a periodic behavior is available, that may serve as a means

of passive attitude stabilization for the spacecraft; coupling effects due to gravity gradient and SRP-induced torques may be cleverly combined to further alleviate the attitude control effort. Virtually, the SRP-induced torque might be not actively compensated; more realistically, ACS will have to control all the perturbations not included in the model, primarily the out-of-plane component of SRP, and those due to the actual motion of the Earth-Moon system with respect to the Sun.

The algorithm used to search a periodic orbit-attitude solution is analogous to the one presented in Section III; when SRP torque is introduced, equation (4) is modified using equation (10), as

$$\dot{\omega}_z = 3K_z \left(\frac{1-\mu}{r_1^3} e_1 e_2 + \frac{\mu}{r_2^3} l_1 l_2 \right) + \frac{\mathbf{T}_{SRP}}{I_z} \qquad (11)$$

Some additional parameters define a dynamical response when a SRP torque is included, namely:

- The area-to-mass ratio A/m;
- At least two of the coefficients C_a, C_s, C_d;
- The position $\mathbf{d}_c$ of the center of pressure;
- The orientation $\hat{n}$ of the Sun-exposed surface in the principal inertia frame.

Furthermore, the moment of inertia I_z appears directly in equation (11), thus the sole inertia ratio K_z is no longer sufficient. Note also that the initial epoch generally dictates the starting Sun angle $\theta_{sun}(0)$, and, therefore, alters the attitude time history.

Mapping the solution space for periodic orbit-attitude behaviors that include SRP, is significantly more complex, because the number of parameters has increased, and it is a large number even in the planar case. Any combination within the parameter set may be virtually employed; the following discussion is an example of spacecraft properties that may be varied to map a portion of the multi-dimensional space of solutions.

Consider to practically construct an orbit-attitude periodic solution that includes SRP. Exploiting a 1:2 Sun-resonant DRO, the correct tuning of the angular velocity $\omega_z(0)$ allows to obtain a periodic attitude behavior, which synchronizes with the apparent Sun motion. The numerical algorithm follows the scheme described in Section III.I; the difference lies in the attitude propagation, which is here performed including SRP torque. At this stage, the solution solely including the gravity gradient torque may be employed as an initial guess.

The resulting motion is visible in Figure 11. The profiles for the angular coordinates are similar, in shape, to those obtained solely considering gravity gradient perturbation, whereas the periodicity of the solution is found each two orbital period. For different resonance ratios (e.g. 1:3, 1:4) periodic solutions may be again obtained, with an attitude behavior that follows the periodicity of the apparent Sun motion.

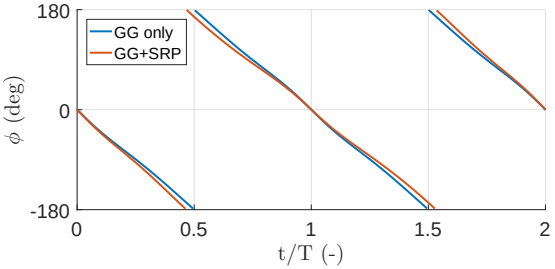

(a) Rotation angle

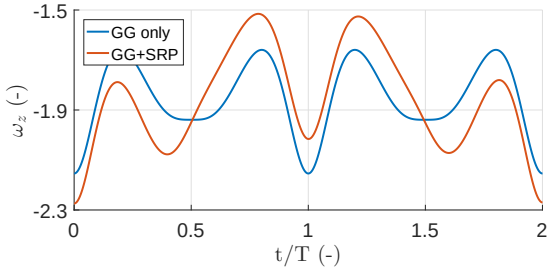

(b) Angular velocity

Figure 11: Sample solution with SRP effect, $K_z = 0.6$, $C_s = 0.4, C_a = 0.6$, 1:2 Sun resonant DRO

Beyond assembling an individual periodic response, it is, also, possible to map the solution space, providing a visual tool to identify an angular velocity that yields periodic attitude motion under SRP. Due to the large variety of parameters that contribute to SRP, a periodicity map only renders a set of all possible solutions along the reference span of orbits (as in Section III); to preserve an easy visualization of the results, it is convenient to create different maps for different parametric sets.

Figure 12 presents the periodicity map for a LSS in a 1:2 Sun-resonant DRO. The lines correspond again to families of periodic orbit attitude solutions; the horizontal axis represents the arm of the SRP force with respect to the center of mass for the spacecraft, and it is directly linked with the magnitude of the SRP torque. The maps are referred to a structure with external dimensions and mass similar to the In-

ternational Space Station (ISS); a large area exposed to solar radiation generates a solution very sensitive to SRP torque. Ultimately, if the distance $|\mathbf{d}_c|$ is large enough, the SRP torque is dominant over the gravity gradient moment. Different inertia ratios are presented in the periodicity maps, to analyze the sensitivity of the solutions to such a parameter.

Figure 13 portrays the periodicity map, referred to the same structure, for a 1:2 Sun-resonant Lyapunov orbit around L_1.

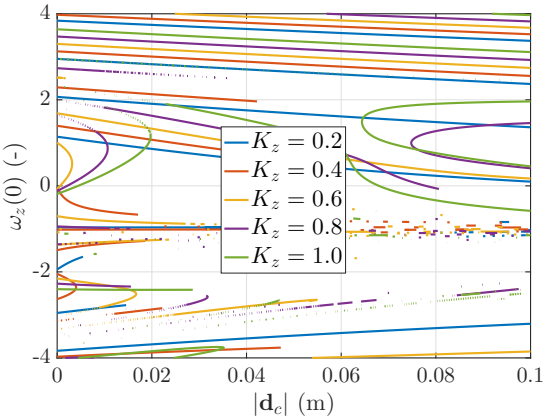

Figure 12: Periodicity map with SRP torque, $C_s = 0.4, C_a = 0.5, A/m = 0.016$, 1:2 Sun resonant DRO

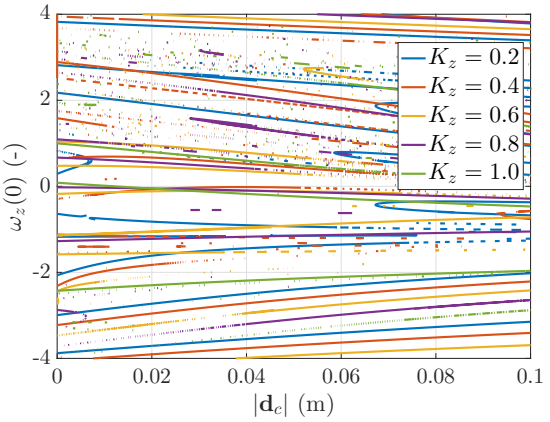

Figure 13: Periodicity map with SRP torque, $C_s = 0.4, C_a = 0.5, A/m = 0.016$, 1:2 Sun resonant L_1 Lyapunov orbit

Note that, the periodicity maps with SRP exhibit a discontinuous behavior, with gaps and scattered lines, due to the increased numerical difficulty in satisfying tolerances after the introduction of SRP torque. In these cases, the algorithm did not converge with the desired tolerance; such solutions might correspond to bounded behaviors, where a quasi-periodic time history is manifested but attitude periodicity is not guaranteed. Further analysis is warranted to clarify the distinction between bounded and periodic solutions, starting from the investigation of discontinuous regions within the solution space.

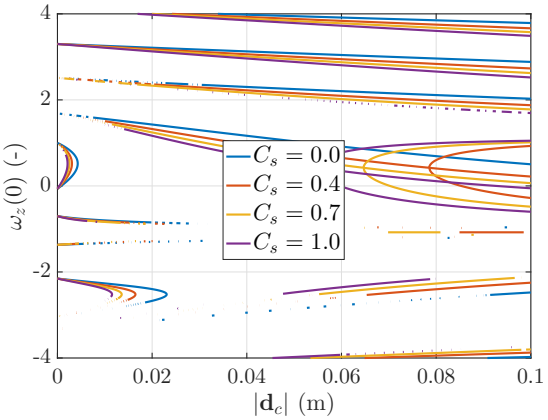

Figure 14: Periodicity map with SRP torque, $K_z = 0.6, C_d = 0, A/m = 0.016$, 1:2 Sun resonant DRO

The sensitivity to other spacecraft parameter may be explored with the same mapping technique, selecting the desired uncertain variable and creating periodicity maps. An additional example of the many possibilities is reported in Figure 14; the set of periodic orbit-attitude solutions on a 1:2 Sun-resonant DRO is mapped, varying the specular reflection coefficient C_s for fixed values of K_z and C_d.

IV.IV Perturbed ephemeris model

The real motion of the Sun with respect to the Earth-Moon system may be introduced as last improvement of the SRP model. The use of ephemeris information to represent the Sun position results in an SRP torque along all the three body axes $\hat{x}_b\hat{y}_b\hat{z}_b$; the orbital motion is still unperturbed within the CR3BP framework.

Such ephemeris model is employed to preliminary investigate the effect of the out-of-plane component of SRP torque, exploring the possible existence of bounded motions. The planar model is convenient to perform the numerical search for periodic behaviors, being aware of the limitations implied in the assumption of coplanar motion for the Sun and Earth-Moon system.

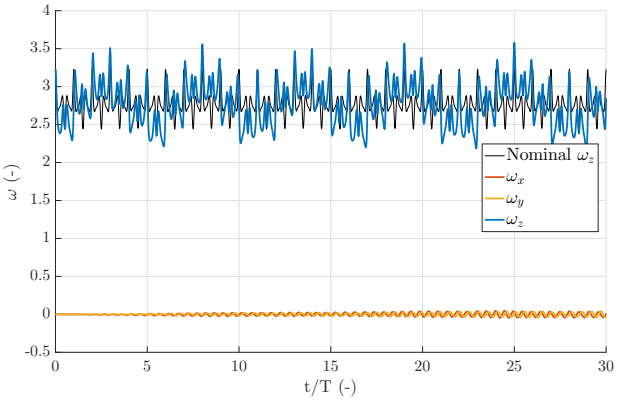

Figure 15: Angular velocity (GG+SRP), using ephemeris for the Sun motion

The small inclination of the Sun orbital motion, relative to the Earth-Moon plane, suggests that the out-of-plane component of SRP may be treated as a perturbation of the nominal planar motion. Figure 15 portrays the angular velocity profile representative of a set of numerical simulations. It is noted that ω_z manifests small oscillations around its nominal profile, thus maintaining the solutions bounded, whereas ω_x and ω_y, responsible for the out-of-plane attitude motion, show a slow increase in magnitude; further long-period analysis will clarify whether the solution remains bounded or have a divergent behavior.

V. Effect of spacecraft flexibility

This Section addresses the dynamics of a flexible spacecraft in the CR3BP environment. Large space structures may possess low structural stiffness and poor structural damping, as far as present, and near-future, materials and technologies are employed. Some low frequency natural modes might, then, be excited by the orbital and rotational motion; in return, flexible vibrations may perturb the vehicle nominal trajectory and/or pointing profile. Effects of this perturbation, in general, appear first as an alteration of the attitude dynamics. Accordingly, this work, first explores how the rotational motion for an actual elastic structure may be different from the nominal rigid body solution, for a fixed reference trajectory.

V.I Model for a flexible structure

A lumped-parameters approach is employed to describe the flexible parts of a spacecraft. Because of the discrete representation for flexible components, lumped-parameters models are in general not able to capture the full dynamical spectrum for an elastic structure. They may, however, be suitable to approximate the first fundamental natural modes.

Presented in [21], Figure 16 portrays the model employed for the analysis: a rigid spacecraft, with inertia moment $\bar{I}_z$, with N_f flexible components attached. Each i-th flexible part is modeled as a Single-Degree-Of-Freedom (SDOF) system, with mass $\bar{m}_i$, stiffness $\bar{k}_i$, connected to the rigid body at the coordinates $\bar{x}_i, \bar{y}_i$. The variable $\bar{s}_i$ indicates the elongation of the i-th spring, and may represent a generic quantity that is associated with a flexible behavior. The angle $\bar{\alpha}_i$ describes the orientation for the i-th SDOF system; for the present investigation, orientation angles, $\bar{\alpha}_i$, are fixed. Let us also denote, with $\bar{\Omega}_i = \sqrt{\bar{k}_i/\bar{m}_i}$, the fundamental frequency of each flexible part.

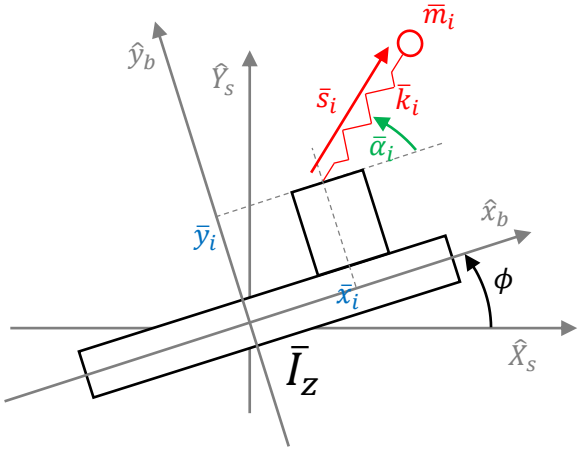

Figure 16: Spacecraft lumped-parameters model

The rotational and vibrational motion are constrained within the $\hat{x}_b\hat{y}_b$ plane, which coincides with the $\hat{X}_s\hat{Y}_s$ plane for the present planar dynamical framework.

V.II Equations of motion

Employing a Lagrangian approach [18, 24], N_f+1 coupled equations of motion are obtained: that is, a set of N_f equations that describe flexible dynamics, plus one equation for rotational dynamics. No external force is assumed to act on the masses $\bar{m}_i$. The gravitational pull of the Earth and the Moon is only applied to the rigid part of the spacecraft, therefore, with null effect on the structural dynamics.

Each SDOF system is governed by the second order differential equation

$$\bar{m}_i\ddot{\bar{s}}_i + (\bar{k}_i - \bar{m}_i\omega_z^2)\bar{s}_i = \bar{m}_i\omega_z^2 L_i - \bar{m}_i\dot{\omega}_z A_i \qquad (12)$$

where two auxiliary coefficients have been defined

$$L_i = (\bar{x}_i \cos\bar{\alpha}_i + \bar{y}_i \sin\bar{\alpha}_i) \tag{13}$$

$$A_i = (\bar{x}_i \sin\bar{\alpha}_i - \bar{y}_i \cos\bar{\alpha}_i) \tag{14}$$

The following equation governs rotational dynamics

$$\dot{\omega}_z \left[\bar{I}_z + \sum_{i=1}^{N_f} \bar{m}_i (\bar{s}_i^2 + \bar{x}_i^2 + \bar{y}_i^2 + 2\bar{s}_i L_i) \right] + \omega_z \sum_{i=1}^{N_f} 2\bar{m}_i (\bar{s}_i \dot{\bar{s}}_i + \dot{\bar{s}}_i L_i) = T_z - \sum_{i=1}^{N_f} \bar{m}_i \ddot{\bar{s}}_i A_i \tag{15}$$

where T_z is the sum of all external torques acting on the spacecraft (e.g., gravity gradient, SRP torque, etc.).

It is interesting to analyze how the attitude dynamics is affected by the structural vibrations; looking at equation (15), observe the followings:

- The first term (between square brackets) represents the overall inertia moment, I_z, of the body, considering both the rigid and the flexible sections;
- The second term is a non-linear coupling term, between the body angular velocity and the linear velocities of the flexible parts;
- The last expression is an equivalent torque, exerted on the spacecraft, due to the inertia forces of the vibrating parts.

V.III Case study: high structural frequencies

It is usually reasonable to assume, for present and near-future space structures, that the orbital and attitude natural frequencies are much lower than the structural ones, i.e.

$$\bar{\Omega}_i \gg \omega_z, \frac{2\pi}{T} \qquad \forall\ i \tag{16}$$

Under such assumption, the behavior of a spacecraft is dominated by the rigid body motion, and the flexible contributions in the left-hand term of equation (15) may be dropped, since they are first or second order infinitesimal quantities [21, 18]. The gyroscopic contribution to stiffness in equation (12) may be neglected too, reducing to

$$\ddot{\bar{s}}_i + \bar{\Omega}_i^2 \bar{s}_i = \omega_z^2 L_i - \dot{\omega}_z A_i \tag{17}$$

It is further assumed that the small flexible vibrations do not significantly perturb the attitude motion, and thus the time history for the spin rate ω_z may be obtained by integration of the rigid body motion, along the orbit, with gravity gradient torque (SRP may be added, too). Having the angular velocity, ω_z, a periodic behavior, equation (17) describes a SDOF, periodically forced system. The resulting problem may be investigated as follows:

1. A rigid body, periodic orbit-attitude solution is obtained, with the techniques described in the previous sections;
2. The time history of ω_z, associated to the rigid body solution (with gravity gradient solely, or GG+SRP), is acquired;
3. The set of N_f equations (17) are solved numerically, or in closed form if the solution for the variable ω_z is approximated with an analytic expansion (e.g. Fourier series);
4. The resulting values $\ddot{\bar{s}}_i$ are employed to compute the attitude perturbation due to vehicle flexibility.

The attitude perturbation within point 4 of the list above is the right-hand term of equation (15), which may be integrated, again, including both external torques and such perturbation. When equation (16) is a valid assumption, the flexibility of the spacecraft does not significantly perturb the attitude motion, resulting in a small, periodic torque with no secular component (as a first approximation in the present framework).

Furthermore, the computation of the coordinates $\bar{s}_i$ may be employed to foresee maximum and mean displacements, and provide preliminary information for structural analysis.

V.IV Case study: low structural frequencies

When structural frequencies are very low, in the neighborhood of the attitude and orbital frequencies, strong coupling may arise between rotational motion, orbital path and vibrations of flexible components. The present Section discusses some results, acknowledging the strong abstraction for the following analysis, and the fact that disposing an highly flexible structure in space is beyond the current technological capability. The sole attitude dynamics is considered, in analogy with the previous Section; the orbital motion may be investigated in future studies.

Dropping the assumption reported in equation (16), the attitude motion needs to be numerically integrated, together with the motion for the flexible

parts. In fact, a non-linear coupling between the elastic displacements and the body angular velocity, i.e., the second term in equation (15), arises, and may be significant in the description of the fully-coupled motion.

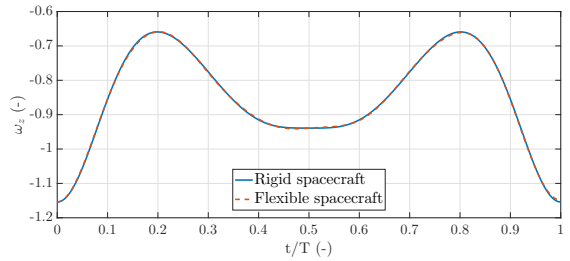

(a) Natural frequencies $\mathcal{O}(10^{-6})$ Hz

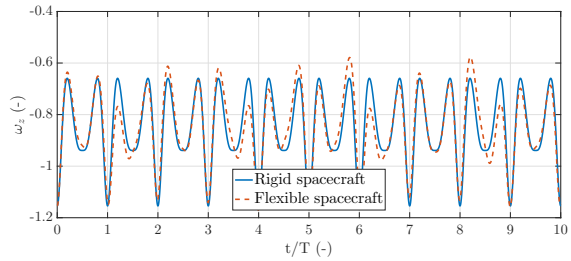

(b) Natural frequencies $\mathcal{O}(10^{-7})$ Hz

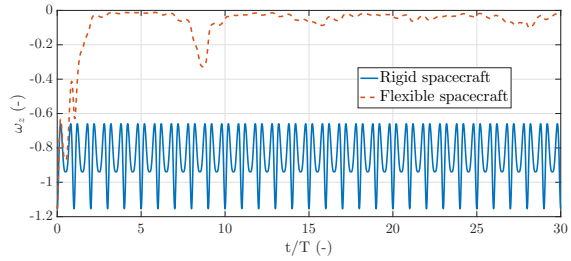

(c) Natural frequencies $\mathcal{O}(10^{-8})$ Hz

Figure 17: Body angular velocity with low structural frequencies $\bar{\Omega}_i$

Figure 17 portrays the angular velocity time history for a spacecraft with lowered structural frequencies; the perturbed attitude profile is displayed together with the nominal solution, that is obtained using a rigid body periodic orbit-attitude solution. The reference orbit is a DRO with period $T = 14.75$ days, which corresponds to a frequency of 7.85×10^{-7} Hz.

As the relative time scaling among the fundamental frequencies for the coupled motion (orbit, attitude, and flexible behaviors) varies, different responses are observed:

- When structural angular frequencies are low with respect to the orbit-attitude motion ones (Figure 17a), the attitude motion encounters small short-period perturbations, which do not hinder the overall behavior; the flexibility of the spacecraft may, thus, be considered as a perturbation of the rigid body attitude solution.

- If structural frequencies are in the neighborhood of the orbital frequency, a strong coupling arises between attitude motion and elastic vibrations. The angular velocity time history (Figure 17b) reveals a strongly non-linear behavior; its periodicity is no longer dominated by the rigid body solution, since large oscillations are due to a flexible structure excitation.

- When structural frequencies are much lower than those of orbital and attitude motion, the elastic components dictate the overall spacecraft behavior. The body angular velocity (Figure 17c) rapidly deviates from the nominal behavior, settling in the neighborhood of zero; accordingly, the movement of the flexible parts is dominant, as their inertia forces attenuate the impact of the gravity gradient torque on the final response.

These observations may be employed for preliminary spacecraft design, to assess the effect of flexible components (e.g. large solar arrays, deployable modules, etc.) on the attitude motion. If the assumption in equation (16) is accurate, the spacecraft dynamics analysis may be based on the rigid body solutions, and flexible behaviors may be treated as small attitude perturbations.

VI. Final remarks

The paper presents a framework to investigate planar orbit-attitude dynamics in both a standard, and a perturbed CR3BP environment.

Periodic solutions, where both orbital and rotational motion are repeated regularly, may be established, assuming the spacecraft to be a rigid body perturbed by gravity gradient torque only. Such solutions are systematically classified into families, and periodicity maps are employed to more efficiently visualize the solution space. These maps may provide the mission analyst a valuable tool for a preliminary analysis, allowing to recognize desired or undesired attitude behaviors without using extensive numerical simulations within complex, higher-fidelity models. The periodic orbit-attitude solutions might offer novel possibilities for future missions involving large

space structures, and the results of the paper may serve as a starting point for further investigations.

The model is, then, refined with the introduction of Solar Radiation Pressure (SRP) torque, combined with a simplified representation of the spacecraft. Artificially fixing the reference orbit, periodic orbit-attitude solutions may still be possible.

Future studies may include the investigation of SRP perturbation on the trajectory, exploring its consequences when both, nominally periodic, orbit and attitude motions are simultaneously perturbed. Novel periodic orbit-attitude solutions may be searched for and explored in the refined model, exploiting the results obtained within the presented assumptions.

Eventually, the perturbation induced on the attitude motion by flexible components is introduced. Such perturbation remains small and bounded as long as the natural frequencies of the flexible structure are much higher than those representative of the orbital attitude motion; when the two sets of natural frequencies possess the same order of magnitude, strong non-linear couplings may emerge, leading to possible diverging behavior. The results are obtained with a lumped-parameters first order model, so further analyses [25] might be devoted to investigate the structural-attitude coupling within a more refined model, which may lead to peculiar behaviors in case of very compliant structures.

References

[1] T. R. Kane and E. L. Marsh, "Attitude Stability of a Symmetric Satellite at the Equilibrium Points in the Restricted Three-Body Problem," *Celestial Mechanics*, Vol. 4, No. 1, 1971, pp. 78–90.

[2] W. J. Robinson, "Attitude Stability of a Rigid Body Placed at an Equilibrium Point in the Restricted Problem of Three Bodies," *Celestial Mechanics and Dynamical Astronomy*, Vol. 10, No. 1, 1974, pp. 17–33.

[3] A. Abad, M. Arribas, and A. Elipe, "On the Attitude of a Spacecraft Near a Lagrangian Point," *Bulletin of the Astronomical Institutes of Czechoslovakia*, Vol. 40, 1989, pp. 302–307.

[4] E. Brucker and P. Gurfil, "Analysis of Gravity-Gradient-Perturbed Rotational Dynamics at the Collinear Lagrange Points," *The Journal of the Astronautical Sciences*, Vol. 55, No. 3, 2007, pp. 271–291.

[5] B. Wong, R. Patil, and A. Misra, "Attitude Dynamics of Rigid Bodies in the Vicinity of the Lagrangian Points," *Journal of Guidance, Control, and Dynamics*, Vol. 31, No. 1, 2008, pp. 252–256.

[6] D. Guzzetti and K. C. Howell, "Coupled Orbit-Attitude Dynamics in the Three-Body Problem: a Family of Orbit-Attitude Periodic Solutions," *AIAA/AAS Astrodynamics Specialist Conference*, 2014.

[7] D. Guzzetti and K. C. Howell, "Natural Periodic Orbit-Attitude Behaviors for Rigid Bodies in Three-Body Periodic Orbits," *66th International Astronautical Congress (IAC)*, 2015.

[8] D. Guzzetti and K. C. Howell, "Natural Periodic Orbit-Attitude Behaviors for Rigid Bodies in Three-Body Periodic Orbits," *Acta Astronautica*, In Press, 2016.

[9] A. J. Knutson, D. Guzzetti, K. C. Howell, and M. Lavagna, "Attitude Responses in Coupled Orbit-Attitude Dynamical Model in Earth–Moon Lyapunov Orbits," *Journal of Guidance, Control, and Dynamics*, Vol. 37, No. 7, 2015, pp. 1264–1273.

[10] A. J. Knutson, *Application of Kane's Method to Incorporate Attitude Dynamics into the Circular Restricted Three-Body Problem.* PhD Dissertation, Purdue University, 2012.

[11] A. J. Knutson and K. C. Howell, "Coupled Orbit and Attitude Dynamics for Spacecraft Comprised of Multiple Bodies in Earth-Moon Halo Orbits," *63rd International Astronautical Congress (IAC)*, 2012.

[12] D. Guzzetti, *Coupled Orbit-Attitude Mission Design in the Circular Restricted Three-Body Problem.* PhD Dissertation, Purdue University, May 2016.

[13] V. Szebehely, *Theory of Orbits: The Restricted Problem of Three Bodies.* Academic Press, New York, 1967.

[14] D. C. Folta, N. Bosanac, D. Guzzetti, and K. C. Howell, "An Earth–Moon System Trajectory Design Reference Catalog," *Acta Astronautica*, Vol. 110, 2015, pp. 341–353.

[15] L. Capdevila, D. Guzzetti, and K. C. Howell, "Various Transfer Options from Earth into Distant Retrograde Orbits in the Vicinity of

the Moon," *AAS/AIAA Space Flight Mechanics Meeting*, 2014.

[16] M. Vaquero and K. C. Howell, "Leveraging Resonant-Orbit Manifolds to Design Transfers Between Libration-Point Orbits," *Journal of Guidance, Control, and Dynamics*, Vol. 37, No. 4, 2014, pp. 1143–1157.

[17] O. C. Winter, "The Stability Evolution of a Family of Simply Periodic Lunar Orbits," *Planetary and Space Science*, Vol. 48, No. 1, 2000, pp. 23–28.

[18] L. Bucci, *Coupled Orbital-Attitude Dynamics of Large Structures in Non-Keplerian Orbits*, MS Thesis, Politecnico di Milano, April 2016.

[19] "Asteroid Redirect Robotic Mission (ARRM) Reference Mission Concept Study Public Information Package V1," 2013.

[20] T. R. Kane, P. W. Likins, and D. A. Levinson, *Spacecraft Dynamics*. McGraw-Hill, New York, 1983.

[21] L. Bucci and M. Lavagna, "Coupled Dynamics of Large Space Structures in Lagrangian Points," *6th International Conference on Astrodynamics Tools and Techniques*, 2016.

[22] J. R. Wertz, *Spacecraft Attitude Determination and Control*. Kluwer Academic Publishers, Dordrecht, 1990.

[23] W. S. Koon, M. W. Lo, J. E. Marsden, and S. D. Ross, *Dynamical Systems, the Three-Body Problem and Space Mission Design*. Springer-Verlag, New York, 2007.

[24] D. Guzzetti, *Large Space Structures Dynamics in a Multi-Body Gravitational Environment*, MS Thesis, Politecnico di Milano, July 2012.

[25] A. Colagrossi and M. Lavagna, "Preliminary Results on the Dynamics of Large and Flexible Space Structures in Halo Orbits," *67th International Astronautical Congress (IAC)*, 2016.